RESEARCH ARTICLE | DECEMBER 04 2023

Structure and absorption behaviour of PAAm-PVA-based nanocomposites reinforced using graphene

Shurooq S. Al-Abbas; Rusul A. Ghazi; Ehssan Al-Bermany ✉; Aqeel Neamah Sarheed; Abdul Kareem J. Albermany

AIP Conf. Proc. 2834, 090056 (2023)
https://doi.org/10.1063/5.0161591

Structure and Absorption Behaviour of PAAm-PVA-Based Nanocomposites Reinforced Using Graphene

Shurooq S. Al-Abbas [1], Rusul A. Ghazi [2], Ehssan Al-Bermany [3,a]), Aqeel Neamah Sarheed[1], Abdul Kareem J. Albermany [4]

[1] *Department of Physics, College of Education for Pure Science, University of Babylon, Babylon, Iraq.*
[2] *Department of Medical Physics, Al-Mustaqbal University College, Babylon, Iraq.*
[3] *Educational Directorate of Najaf, Ministry of Education, Najaf, Iraq.*
[4] *Department of Physiology and Medical Physics, College of Medicine, Babylon, Iraq.*

[a)] corresponding author: ehssan@itnet.uobabylon.edu.iq

Abstract. Doping with graphene nanosheets has attracted significant interest from researchers to enhance the structure and properties of nanomaterials because of graphene's unique properties and broad and essential applications. The study aims to focus on the effect of functional groups of both polymers and nanomaterials to fabricate a new nanocomposite consisting of poly (acrylamide) (PAAm) with poly (vinyl alcohol) (PVA) before and after the addition of graphene oxide nanosheets (GO) and studying its structural and optical properties. The developed method (dissolving with water, mixing, sonication, and casting) showed success in fabricating new nanocomposites for the first time by mixing these components with a ratio of 4.5: 4.5: 1 as percentages (PAAm: PVA: GO). Samples showed homogeneity of the polymer mixtures with each other and the excellent dispersion of graphene oxide nanosheets in the new polymer nanocomposite as exhibited by optical microscopy. The spectra of the Fourier infrared spectroscopy showed the strong interfacial interaction of the two polymers in the polymeric mixture with GO nanoparticles as nanocomposites. Also, X-ray diffraction showed shifting in some peak positions and increased crystallization of the polymers in the nanocomposites. The nanocomposites showed a notable improvement in the optical properties due to doping the polymeric mixture with graphene oxide compared with their blended polymers. The energy gap also significantly decreased after the contribution of graphene oxide up to 136% and 900% for the permitted and prohibited direct transfers, respectively. These results exposed promising nanocomposites for widespread applications such as solar cells.

Keywords: PAAm, PVA, GO, functional group, optical properties, bandgap nanocomposites.

INTRODUCTION

Nanocomposites based-polymer fabrication is impacted by several factors, such as interaction, loading transfer homogeneity, functional group, partial size, and dispersion in the polymer matrix, etc. (1,2). The Functional surface group of materials could bring significant importance to succeed in great improvements, performance, and achieving new properties of the nanocomposites that are different from the original component properties (3). In addition, it could bring stability to the nanomaterials after loading in the matrix and could significantly improve the properties of polymer nanocomposites (4). Experiments investigation have been carried out to achieve the homogeneity, good dispersion, interactions, and compatibility of nano-fillers loaded in the nanocomposite matrix (5). Therefore, getting a homogeneous sample with good interfacial interaction is essential to improve properties that apply the functional group in the matrix or nanofillers (6). This important factor is not fully understood, and limited studies focused on or reported this issue.

Nanotechnology has a wide range of technology that can significantly understand the interaction between the materials (7). In contrast, nanotechnology is concerned with the technology used to administer material at the atomic level to fabricate new nanomaterials with various properties (8). The surface area to volume ratio is high in nanomaterials. Therefore the physicochemical qualities may vary depending on the shape and size. Nanomaterials characterize different physicochemical properties by the nanoparticles such as graphene nanosheets. Graphene is a thin carbon atom with a 2D network (9), optical transparency, and absorption properties (10). The surface of graphene oxide (GO) is abundant in the functional groups (11) that turn GO hydrophilic and capable of strong interactions. These functional groups are associated with better distribution and acceptable interactions among the components in the matrix to form better nanocomposites (12). The

2nd International Conference of Mathematics, Applied Sciences, Information and Communication Technology
AIP Conf. Proc. 2834, 090056-1–090056-12; https://doi.org/10.1063/5.0161591
Published by AIP Publishing. 978-0-7354-4715-8/$30.00

unique features of GO make it very interesting in wide and several applications such as solar cells, nano-electronics, sensors, supercapacitors, and medicine (13).

Polyacrylamide (PAAm) is a water-soluble polymer and does not resemble a monomer; non-toxic because the proportion of nitrogen is 19.7%, and the percentage of hydroxyl groups is 3.6% (14). It is usually doped to enhance the water viscosity (15). This polymer can be used in various applications, including water treatment, mining, and oil recovery. Recently, it has been used in surface grafting polymerization (16). Also, PAAm is used as a thickening agent for materials, as flocculants, artificial corneas, and in the manufacture of burns as tissue covering (14,15)

Luo, YL et al. (17) fabricated and characterized PVA/PAAm that loaded with the copper nanoparticles to fabricated nanocomposites of hydrogels materials. Copper nanoparticles are well distributed in PVA - PAAm with a spherical architecture with a particle size ranging between (11.5) nm to (20) nm, characterized using XRD and UV-vis spectroscopy. A complex interaction between Cu^{2+} ions with -OH groups in PVA and amid - carbonyl groups in PAAm is reported as an essential factor that impacts the results. B. C. Yadav et al. (18) studied the fabricated of zinc (II) nitrate-polyacrylamide (PAAm) film on a substrate for optoelectronic application and humidity sensing. The findings and outcomes were also favorable. The sensor's sensitivity was recorded at 1.813 W/ percent RH. The substance can be replicated 96 percent of the time that can be stable for more than 14 days. Response and recovery times were recorded at (250) and (37) seconds, respectively. These results are utilized as an optoelectronic humidity sensor and can be employed in remote locations and unattended stations because of their optical properties. Büşra Osma et al. (19) considered the impact of the GO and temperature on the swelling of PAAm-GO nanocomposites gel. The findings of this work suggest that the fluorescence approach can be utilized to trace the kinetics of the PAAm-swelling GO composite in water at various temperatures and GO content. This technique calculated the swelling time constants and cooperative diffusion coefficients for composite gels made with PAAm and different GO contents. It is important to note that the GO component may work as a multifunctional cross-linker, forming more PAAm- GO composite junctions and increasing crosslink density, lowering swelling power.

There are few studies on these polymers and their characterization. In addition, no study reported these materials with graphene as nanocomposites. Therefore, this study focused on fabricated new samples loaded with graphene oxide nanosheets. Also, the GO impacts on the structure and optical properties of (PAAm-PVA) blended polymers and (PAAm-PVA/GO) nanocomposite films are exhibited. These polymers have never been considered with graphene, or one of them is derivative.

EXPERIMENTAL PART

The Utilized Materials

Full details of raw materials are concise in Table (1).

TABLE 1. The details of used materials.

Raw materials	Details	Supplier	Country
Polyvinyl alcohol (PVA)	(160 *10^3 g mol^{-1}) Mw	Dindori,	Nashik, India
Polyacryl amide (PAAm)	(5 to 30 10^6 $g.mol^{-1}$) Mw, (1.13 g/cm^3), density, and (6-8) PH Level.	Shenzhen sendi	Biotechnology Co. Ltd, China
Graphene oxide (GO)	Handmade, by E. Al-Bermany (1).	At the University of Sheffield	The UK

Sample Purification

Full details of sample purification were shortened in Table (2).

TABLE 2. The sample purification.

Sample	Concentration wt. %			Details
	PVA	PAAm	GO	
PAAm-PVA	**50**	**50**	**0**	Polymer dissolved in distilled water after stirring for 1/2 hour, then sonication for 15 minutes each 12 hours. This procedure was repeated for 72 hours. Then GO was added to samples then another 72 hours of mixing using the same method. Finally, the samples were cast in a Petri dish and dried under air for final films.
PAAm-PVA/GO	**4.5**	**4.5**	**1**	

Characterization

Characterization details are illustrated in Table (3).

TABLE 3. Characterizations used.

Device	Model	Details	Manufacturing and Country
Fourier transforms infrared spectroscopy (FTIR)	vertex 70	Measurements range between 4000 -500 cm^{-1}	Bruker, Germany
Optical microscope (OM)	Model 73346, Nikon	Magnification	Olympus, Japan
XRD Diffraction	Xpert		Phillips, Holland
UV-Visible spectrophotometer	Shimadzu, UV-1800A^{o}	Double Beam	Phillips, Japan

RESULTS AND DISCUSSIONS

The samples' FT-IR spectra with IR region (4000-500 cm-1) were recorded, as exposed in Figure (1). The FTIR spectrum of PAAm-PVA displayed several functional group peaks at 3285 cm^{-1} of the hydroxyl (O-H) group, 2940 cm^{-1} of the methylene (C-H), 1715 cm^{-1} carboxyl acid (C=O) stretch, 1644 cm^{-1} of the amide group, 1258 cm^{-1} of the (O-H) hydroxyl group, and 1087 cm^{-1} of the (C-O-C) epoxy group cm^{-1}. The spectra of the nanocomposites exposed the same polymer peaks within a shifting in the position peaks such as (2946 to 2940, 1715 to 1706, 1660 to 1650, and 1266 to 1258) cm^{-1} respectively, compared to PAAm-PVA blended polymer. This might be associated with the strong hydrogen interfacial interaction among the polymers functional groups and GO functional groups, with other research findings (20,21).

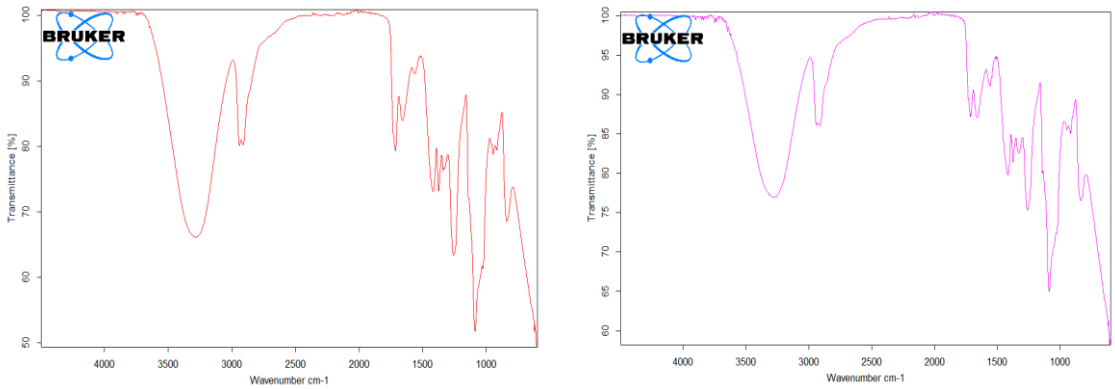

(a) (b)

FIGURE 1. FTIR spectra of a) blended polymers and b) nanocomposite films.

Figure (2) demonstrates the XRD patterns of the sample films. Interestingly, these blended polymers exhibited a different structure. The PAAm-PVA spectra showed peaks at 2θ = 32.08°, 45.79°, 56.93°, 66.66°, and 75.74° related to PAAm in agreement with the literature (20,22). The samples also display the minor feature of the peak of PVA at 2θ = 19.9°, in accord with the literature (23). The addition of GO in the PAAm-PVA/GO exhibited a slight shifting to higher values in the peak positions, such as 32.21° to 32.08° and from 45.79° to 45.91°, respectively, compared to PAAm-PVA blended polymer.

Moreover, the intensity of the peaks changed after adding GO but did not affect the polymer structure in the nanocomposite films in similar behavior to other literature (1). The XRD results were backed up by FTIR results, revealing a strong connection between GO nanosheets and the matrix blended polymers.

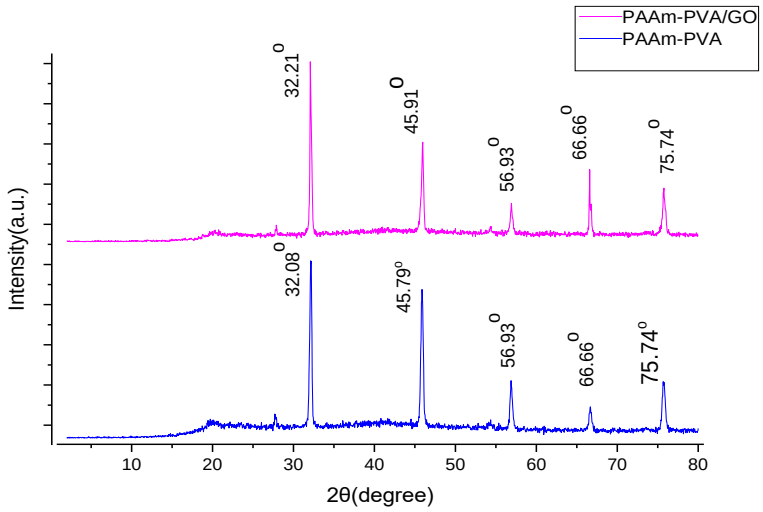

FIGURE 2. XRD patterns of sample films.

The crystalline size (D) was valued in (nm) using the Scherer equation (6).

$$D = \frac{K\lambda}{\beta cos\,(\theta)} \tag{1}$$

Where K, β, $FWHM$, λ, and θ are factors average crystallite = ~0.9, the full width of the crystalline peaks at half-maximum of the material, and X-ray incident wavelength (nm), and Bragg angle. The nanocomposite results revealed an increase in crystallinity due to the contribution of the GO nanosheets compared with the blended polymer, as shown in Table 4.

TABLE 4. The average crystallite size of sample films.

Samples	Peaks			
	1	**2**	**3**	**4**
PAAm-PVA	4.509	3.675	3.887	**4.048**
PAAm-PVA/GO	6.017	4.564	3.943	**8.546**

Figure (3) illustrates the OM images sample films. These images displayed the smooth surface of the samples that presented a fine homogenous between the blended polymer, as shown in Figure (3 a). Meanwhile, the GO nanomaterials have an excellent dispersion in the polymer matrix of the PAAm-PVA/ GO nanocomposite films without any aggregation, as revealed in Figure (3 b).

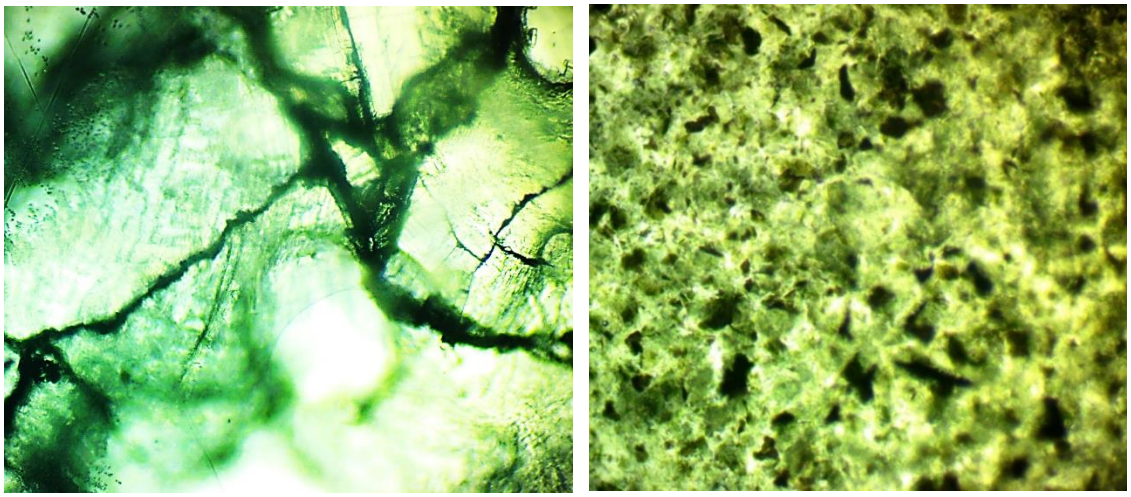

(a) **(b)**

FIGURE 3. The OM images of a) PAAm-PVA with the magnification (100 X) and b) PAAm-PVA/GO nanocomposite with the magnification (40X).

Absorption (A) is the ratio between the light intensity (I_A) and the incident light (I_o) of a material (24).

$$A = \frac{I_A}{I_0} \quad (2)$$

UV-irradiation of PAAm-PVA and the PAAm-PVA/GO nanocomposite in the wavelength region (200-1200) nm in Figure (4). The cross-linked polymer peaks then explained the slow study behavior. Interestingly, the PAAm-PVA blended polymer has lower absorbance than the PAAm-PVA/GO nanocomposite (17). The transitions are shown absorption peaks in the wavelength region at 200 nm and 280 nm, resulting from the π-π transition of blended polymers and graphene oxide nanoparticles, respectively. GO nanosheets caused an improvement in the absorbance of the material related to the ability of GO nanosheets that absorb 2.3% for every single sheet over a broad wavelength range. These nanocomposite results could be suitable for optoelectronic applications (25).

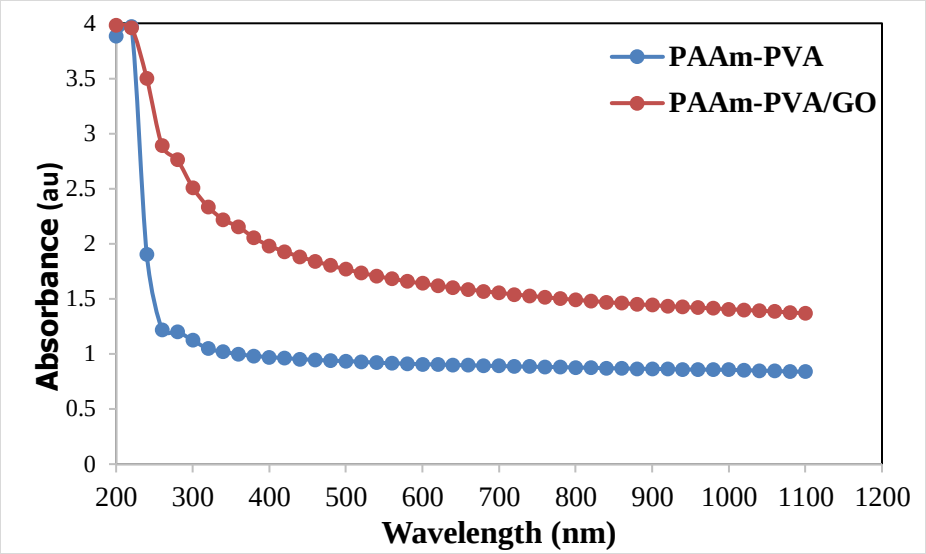

FIGURE 4. Absorption spectra of blended polymers and nanocomposite films with the wavelength.

Figure (5) presents the absorption coefficient (α) with a photon energy of the PAAm-PVA polymeric mixture and the PAAm-PVA-GO nanocomposite mixture that is considered using the Lambert bear equation (26).

$$\alpha = 2.303\, A/t \tag{3}$$

The absorption tends to improve gradually with increasing the photon energy, which indicates the electron transitions were increased. Interestingly, the nanocomposite presented a higher adsorption coefficient behavior than blended polymers. The incorporation of graphene oxide nanosheets is associated with an enhanced absorption coefficient compared to the composite polymers. Moreover, blended polymer showed the lowest absorption coefficient at higher photon energy than nanocomposite. Graphene has impressive and unique optical transportation (27,28) with a substantial amount of the sp^2 hybridized and carbon backbone structure that turns GO to a high planarity degree (29) with a large surface area (30). These unique properties helped to this achievement.

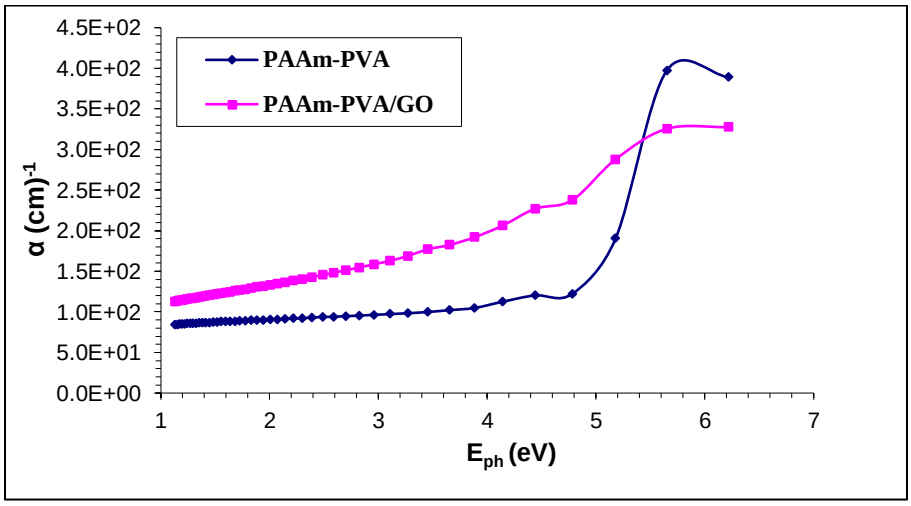

FIGURE 5. The coefficient of absorption with the photon energy of sample films.

Figure (6) displays the extinction coefficient (k) of the samples with the wavelength calculated from the following equation (31,32).

$$K = \frac{\alpha\lambda}{4\pi} \quad (4)$$

Where, (λ = 1.5406) Aº, the wavelength straight of the Cu Kα. The extinction coefficient of the nanocomposite improved compared to the blended polymer. Moreover, graphene oxide nanosheets can change the composition of the host mixture (PAAm-PVA), where GO showed a significant impact associated with improving the absorption, thus enhancing the extinction coefficient. In addition, the absorption and extinction coefficients have a related relationship according to equation (6). Also, this finding agreed with other results in the works of literature (33).

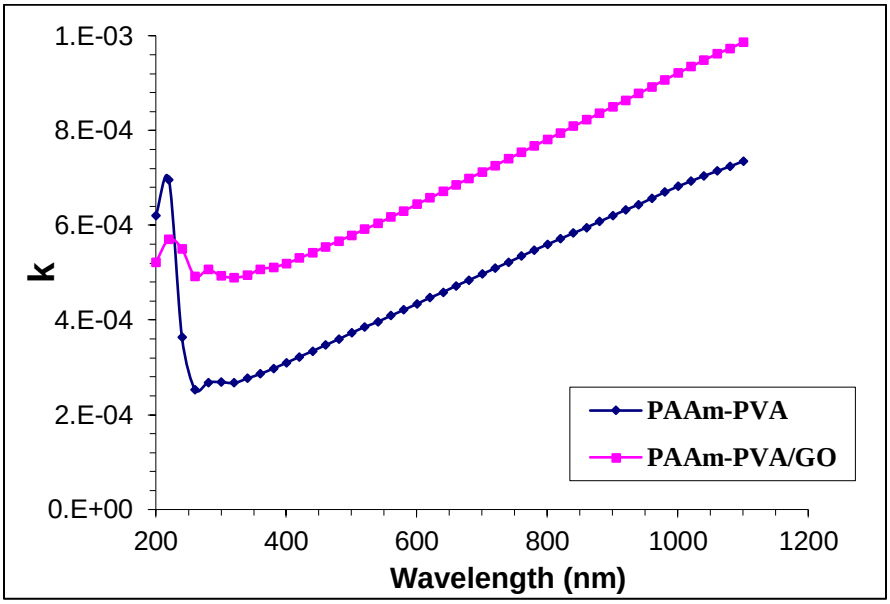

FIGURE 6. Extinction factor of blended polymers and nanocomposite films with the wavelength.

The dielectric constant (real and imaginary) was calculated for the samples using equations (6) and (7), respectively (31).

$$\varepsilon = \varepsilon_r + \varepsilon_i \quad (5)$$
$$\varepsilon_r = n^2 - k^2 \quad (6)$$
$$\varepsilon_i = 2nk \quad (7)$$

Where ε_r and ε_i mean the real and imaginary dielectric constant parts, respectively, Figure (7) shows a sharp increase of the real dielectric constant (ε_1) at lower wavenumbers. The nanocomposite results exhibited better improvement and continued to increase instead of the effects of blended polymer that were reduced.
Figure (8) demonstrates the imaginary dielectric constant (ε_2) and the wavelength of the polymer blended and nanocomposite (PAAm-PVA) (PAAm-PVA/GO); it was noticed from the results that the (ε_2) enhanced with the increase in the wavenumber because the values of the imaginary dielectric constant depend on the changes in the value of the coefficient of absorption (6). Meanwhile, adding GO graphene oxide nanosheets should significantly improve the nanocomposite. This is because the growth of the electrical polarization in the samples after adding the graphene oxide nanostructures also improved the real and theoretical dielectric constants, consistent with the literature (34,35).

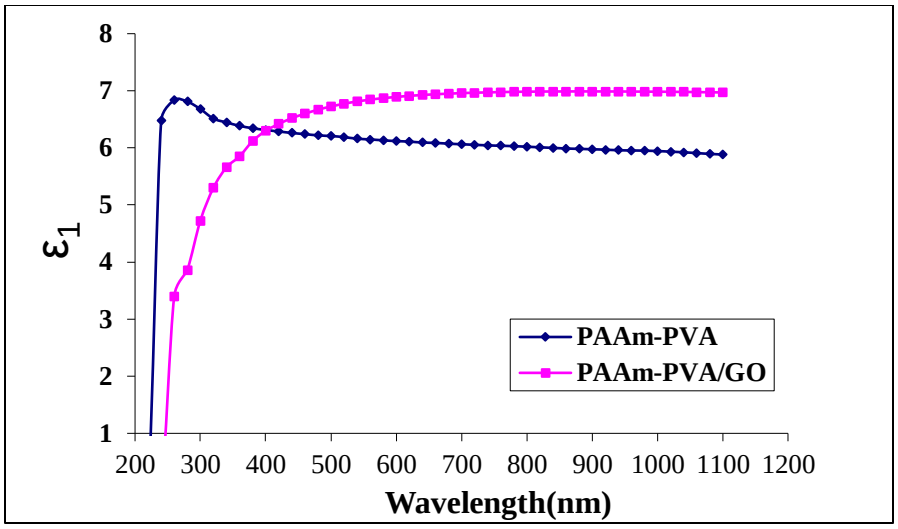

FIGURE 7. The real dielectric constant of the blended polymers and nanocomposite films with the wavelength.

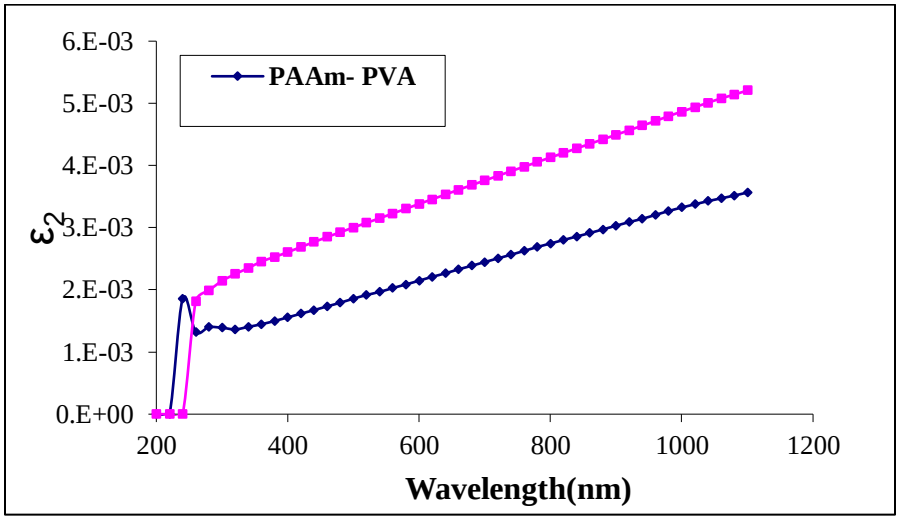

FIGURE 8. The imaginary dielectric constant of the blended polymers and nanocomposite films with the wavelength.

Equation (8) was used to calculate the allowed and indirect optical energy gap by drawing the interception of the extrapolated linear component with the photon energy at $(\alpha h\nu)^{1/n} = 0$ (24).

$$ahv = B\,(hv - E_g)^r \tag{8}$$

Where (B) is constant, (h) Planck's constant, (v) frequency, (E_g) phonon energy, and (r) the exponential constant, which represent various values depending on the transition forms such as (1/2 or 3/2), or (2 or 3) for allowed or forbidden direct, or indirect, respectively (31). The energy gap value of both transmissions was considered by drawing the graph between $(\alpha h\upsilon)^{1/2}$ with the photon energy $(h\upsilon)$, as exhibited in Figure (9) and Figure (10), respectively. The photon energy axis $(\alpha h\upsilon=0)^{1/2}$ revealed the finding of the indirect energy gap, where the values of the energy gap were reduced after the contribution of GO, where the nanomaterials associated with the displacement of the absorption edge to low energies, where reduced the energy gap designates the development of new local levels that is below the conduction band and above the valence bands in the forbidden gap. Where the optical energy gap is affected by the prepared films' preparation conditions and structure (6).

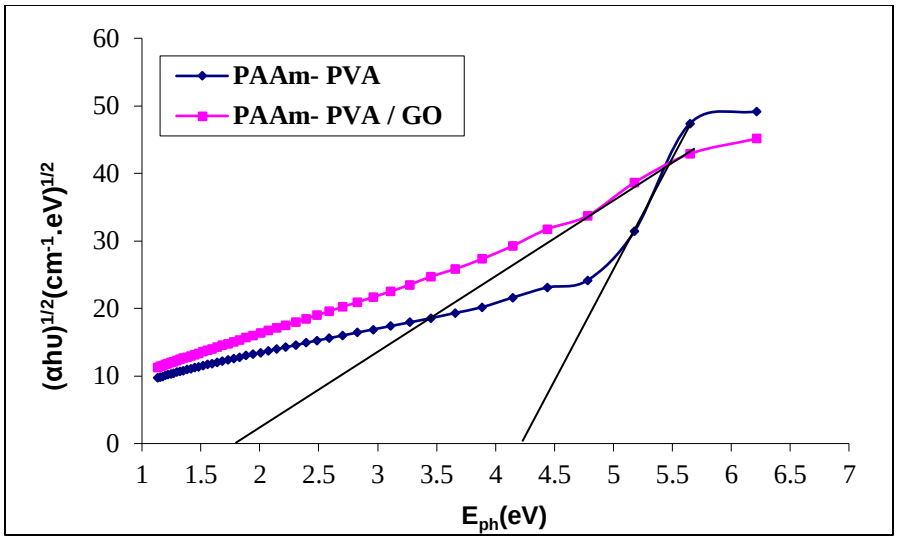

FIGURE 9. The optical energy gap for the allowed direct transition $(\alpha h\upsilon)^{1/2}$ with the photon energy of sample films.

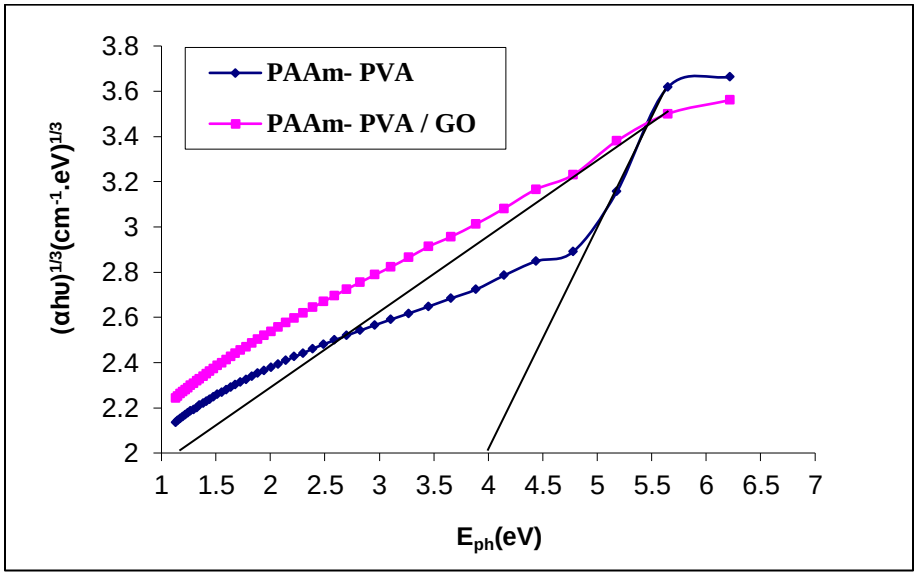

FIGURE 10. The optical energy gap of the forbidden direct transition of sample films with the photon energy.

Therefore, this behavior was significantly improved after adding GO nanosheets, as the energy gap of the nanocomposites decreased to displayed values of less than 0.5 eV of the energy gap compared to the polymeric mixture, as revealed in Table (5). At the same time, GO assisted in improving and outstandingly reducing the energy gap values. As a result, the polymeric mixture was transformed into semiconductor materials for nanocomposites. The bandgap showed a significant improvement of 136% for the allowed transition and 900% for the prepared transition compared with the polymeric mixture.

TABLE 5. The optical energy gap of samples.

Sample Code	Direct Transition (eV)	
	Allowed	Forbidden
PAAm-PVA	4.25	4
PAAm-PVA/GO	1.8	0.4

The refractive index (n) was found from the relationship (9) (32,36).

$$n = \frac{1+R}{1-R} + \left[\frac{4R}{(1-R)} - K^2\right]^{1/2} \quad (9)$$

(R) is the reflectance. The change in the refractive index of the polymer blended and nanocomposite with the wavelength is illustrated in Figure (11). In the ultraviolet region, the refractive index results in a sharp increase in both samples. In contrast, in the visible area, the blended polymer values were gradually reduced while the nanocomposite's behavior was progressively improved. Interestingly, the nanocomposite presents outstanding ability and increases to adsorb the ray after loading the GO without loss in the optical transparency of the nanocomposites (37). This finding is related to the unique properties such as high optical transmittance in the visible spectrum of graphene nanosheets, in addition to the high mobility of the carrier and high electric conductivity (38).

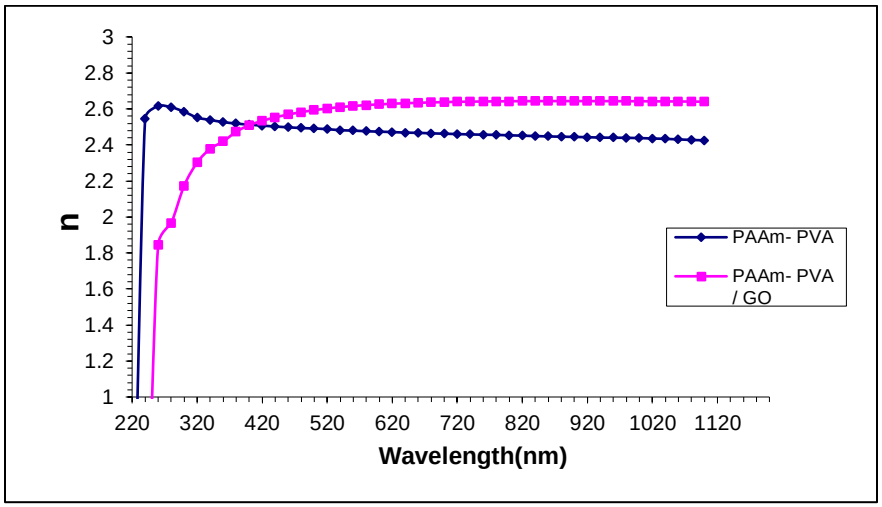

FIGURE 11. The refractive index (n) of blended polymers and nanocomposite films with the wavelength.

CONCLUSIONS

The new nanocomposite was effectively fabricated and characterized, as shown by FTIR, XRD, and OM images. FTIR shows a strong and strong interfacial interaction among blended polymers with the nanosheets of GO. In addition, OM images of the samples exhibited suitable homogeneous and fine nanomaterials dispersed without any aggregation or loss of transparency. The involvement of GO showed a substantial improvement in the structural and optical properties compared to the blended polymer film .The energy gap improved to 136% and 900% for the real and imaginary direct transfers, respectively, after the loading of graphene oxide. This showed samples with high absorption and good transparency that could be promising in solar cell applications.

REFERENCES

1. Al-Bermany E, Chen B. Preparation and characterization of poly(ethylene glycol)-adsorbed graphene oxide nanosheets. Polymer International. 2021;70(3):341–51.
2. Díez-Pascual AM, Gómez-Fatou MA, Ania F, Flores A. Nanoindentation in polymer nanocomposites. Progress in Materials Science [Internet]. 2015 Jan;67:1–94. Available from: https://linkinghub.elsevier.com/retrieve/pii/S0079642514000553
3. Al-shammari AK, Al-Bermany E. Polymer functional group impact the thermo-mechanical properties of polyacrylic acid, polyacrylic amide- poly (vinyl alcohol) nanocomposites reinforced by graphene oxide nanosheets. Journal of Polymer Research [Internet]. 2022 Aug 29;29(8):351. Available from: https://link.springer.com/10.1007/s10965-022-03210-3
4. Layek RK, Nandi AK. A review on synthesis and properties of polymer functionalized graphene. Polymer [Internet]. 2013 Aug;54(19):5087–103. Available from: https://linkinghub.elsevier.com/retrieve/pii/S0032386113005636
5. Cui M, Park S-J, Kim S. Carboxylated Group Effect of Graphene Oxide on Capacitance Performance of Zr-Based Metal Organic Framework Electrodes. Journal of Inorganic and Organometallic Polymers and Materials [Internet]. 2021;31(5):1939–45. Available from: https://doi.org/10.1007/s10904-021-01935-0
6. Kadhim MA, Al-Bermany E. New fabricated PMMA-PVA/graphene oxide nanocomposites: Structure, optical properties and application. Journal of Composite Materials [Internet]. 2021 Aug 3;55(20):2793–806. Available from: http://journals.sagepub.com/doi/10.1177/0021998321995912
7. Krystek M, Górski M. Nanomaterials in Structural Engineering. In: New Uses of Micro and Nanomaterials. 2018.
8. Kolahalam LA, Kasi Viswanath I V., Diwakar BS, Govindh B, Reddy V, Murthy YLN. Review on nanomaterials: Synthesis and applications. In: Materials Today: Proceedings. Elsevier Ltd.; 2019. p. 2182–90.
9. Yang G, Li L, Lee WB, Ng MC. Structure of graphene and its disorders: a review. Vol. 19, Science and Technology of Advanced Materials. Taylor & Francis; 2018. p. 613–48.
10. Lee C, Wei X, Kysar JW, Hone J. Measurement of the Elastic Properties and Intrinsic Strength of Monolayer Graphene. Science. 2008;321(18 JULY):385–8.
11. Abdul kadhim M, Al-bermany E. Enhance the Electrical Properties of the Novel Fabricated PMMA-PVA/ Graphene Based Nanocomposites. Journal of Green Engineering. 2020;10(7):3465–83.
12. Al-Abbas SS, Ghazi RA, Al-shammari AK, Aldulaimi NR, Abdulridha AR, Al-Nesrawy SH, et al. Influence of the polymer molecular weights on the electrical properties of Poly(vinyl alcohol) – Poly(ethylene glycols)/Graphene oxide nanocomposites. Materials Today: Proceedings [Internet]. 2021;42(5):2469–74. Available from: https://linkinghub.elsevier.com/retrieve/pii/S2214785320402822
13. Jo H, Sim M, Kim S, Yang S, Yoo Y, Park J-H, et al. Electrically conductive graphene/polyacrylamide hydrogels produced by mild chemical reduction for enhanced myoblast growth and differentiation. Acta Biomaterialia [Internet]. 2017 Jan;48:100–9. Available from: https://linkinghub.elsevier.com/retrieve/pii/S174270611630561X
14. Al-shammari AK, Al-Bermany E. New Fabricated (PAA-PVA/GO) and (PAAm-PVA/GO) Nanocomposites: Functional Groups and Graphene Nanosheets effect on the Morphology and Mechanical Properties. Journal of Physics: Conference Series [Internet]. 2021 Aug 1;1973(1):012165. Available from: https://iopscience.iop.org/article/10.1088/1742-6596/1973/1/012165
15. Billmeyer FW. Textbook of Polymer Science. Kobunshi. 1963;12(3):240–51.
16. Amini-Fazl MS, Barzegarzadeh M, Mohammadi R. Surface Modification of Graphene Oxide with Crosslinked Polymethacrylamide via RAFT Polymerization Strategy: Effective Removal of Heavy Metals from Aqueous Solutions. Journal of Inorganic and Organometallic Polymers and Materials [Internet]. 2021;31(7):2959–70. Available from: https://doi.org/10.1007/s10904-021-01918-1
17. Luo YL, Chen LL, Xu F, Feng QS. Fabrication and characterization of copper nanoparticles in PVA/PAAm IPNs and swelling of the resulting nanocomposites. Metals and Materials International. 2012;18(5):899–908.
18. Yadav BC, Sikarwar S, Yadav R, Chaudhary P, Dzhardimalieva GI, Golubeva ND. Preparation of zinc (II) nitrate poly acryl amide (PAAm) and its optoelectronic application for humidity sensing. Journal of Materials Science: Materials in Electronics. 2018;29(9):7770–7.
19. Osma B, Evingür GA, Pekcan Ö. Effect of temperature and graphene oxide on the swelling of PAAm-

GO composite gels. Proceedings of the World Congress on New Technologies. 2019;0:6–10.
20. Deshmukh K, Ahmad J, Hägg MB. Fabrication and characterization of polymer blends consisting of cationic polyallylamine and anionic polyvinyl alcohol. Ionics. 2014;20(7):957–67.
21. Aldulaimi NR, Al-Bermany E. New Fabricated UHMWPEO-PVA Hybrid Nanocomposites Reinforced by GO Nanosheets: Structure and DC Electrical Behaviour. Journal of Physics: Conference Series [Internet]. 2021 Aug 1;1973(1):012164. Available from: https://iopscience.iop.org/article/10.1088/1742-6596/1973/1/012164
22. El-Gamal S, El Sayed AM. Physical properties of the organic polymeric blend (PVA/PAM) modified with MgO nanofillers. Journal of Composite Materials. 2019;53(20):2831–47.
23. Yang CC. Chemical composition and XRD analyses for alkaline composite PVA polymer electrolyte. Materials Letters. 2004;58(1–2):33–8.
24. Pankove JI, Kiewit DA. Optical Processes in Semiconductors. Journal of The Electrochemical Society [Internet]. 1972;119(5):156C. Available from: https://iopscience.iop.org/article/10.1149/1.2404256
25. Lewis CE. The training of new health manpower. Academic Medicine [Internet]. 1975 Dec;50(12):75–83. Available from: http://www.ncbi.nlm.nih.gov/pubmed/503
26. Alias AN, Zabidi ZM, Ali AMM, Harun MK, Yahya MZA. Optical Characterization and Properties of Polymeric Materials for Optoelectronic and Photonic Applications. International Journal of Applied Science and Technology [Internet]. 2013;3(5):11. Available from: https://www.ijastnet.com/journals/Vol_3_No_5_May_2013/3.pdf
27. Kim KS, Zhao Y, Jang H, Lee SY, Kim JM, Kim KS, et al. Large-scale pattern growth of graphene films for stretchable transparent electrodes. Nature. 2009;457:706–10.
28. Tetsuka H, Asahi R, Nagoya A, Okamoto K, Tajima I, Ohta R, et al. Optically tunable amino-functionalized graphene quantum dots. Advanced Materials. 2012;24(39):5333–8.
29. Hong BJ, Compton OC, Zhi An IE, Nguyen ST. Successful Stabilization of Graphene Oxide in Electrolyte Solutions: Enhancement of Bio-functionalization and Cellular Uptake. ACS Nano. 2012;6(1):63–73.
30. Compton OC, Nguyen ST. Graphene oxide, highly reduced graphene oxide, and graphene: Versatile building blocks for carbon-based materials. Small. 2010;6(6):711–23.
31. Suryawanshi VN, Varpe AS, Deshpande MD. Band gap engineering in PbO nanostructured thin films by Mn doping. Thin Solid Films [Internet]. 2018 Jan;645:87–92. Available from: https://linkinghub.elsevier.com/retrieve/pii/S0040609017307678
32. Ingham JD, Lawson DD. Refractive Index-Molecular Weight Helatlonships. Journal of Polymer Science. 1965;A3(7):2707–10.
33. Aldulaimi NR, Al-Bermany E. Tuning the bandgap and absorption behaviour of the newly-fabricated Ultrahigh Molecular weight Polyethylene Oxide- Polyvinyl Alcohol/ Graphene Oxide hybrid nanocomposites. Polymers and Polymer Composites [Internet]. 2022 Jan 29;30:096739112211121. Available from: http://journals.sagepub.com/doi/10.1177/09673911221112196
34. Al-Owaedi OA, Khalil TT, Karim SA, Said MH, Al-Bermany E, Taha DN. The promising barrier: Theoretical investigation. Systematic Reviews in Pharmacy. 2020;11(5):110–5.
35. Abdelamir AI, Al-Bermany E, Sh Hashim F. Enhance the Optical Properties of the Synthesis PEG/Graphene- Based Nanocomposite films using GO nanosheets. Journal of Physics: Conference Series [Internet]. 2019 Sep 1;1294(2):022029. Available from: https://iopscience.iop.org/article/10.1088/1742-6596/1294/2/022029
36. Ghazi RA, Al-mayalee KH, Al-bermany E, Hashim FS, Albermany AKJ. Impact of polymer molecular weights and graphene nanosheets on fabricated PVA-PEG / GO nanocomposites : Morphology , sorption behavior , and shielding application. AIMS Materials Science. 2022;9(4):4.
37. Schadler L. Model interfaces. Nature Materials [Internet]. 2007 Apr;6(4):257–8. Available from: http://www.nature.com/articles/nmat1873
38. Li D, Müller MB, Gilje S, Kaner RB, Wallace GG. Processable aqueous dispersions of graphene nanosheets. Nature Nanotechnology [Internet]. 2008 Feb 27;3(2):101–5. Available from: http://www.nature.com/articles/nnano.2007.451